Eur. Phys. J. Spec. Top.
https://doi.org/10.1140/epjs/s11734-025-01713-w

THE EUROPEAN PHYSICAL JOURNAL SPECIAL TOPICS

Regular Article

Stretchable self-sensing conductive hydrogel with tunable photothermal response and actuation capability

Ping Guo[1], Yingqiang Zhou[2], Wenjie Cao[1], Xinyin Wang[1], Tian Wang[1], Hongxiang Su[1], Lin Cheng[1], Huaping Wu[3], Long Li[4,a], and Aiping Liu[1,b]

[1] Zhejiang Key Laboratory of Quantum State Control and Optical Field Manipulation, Department of Physics, Zhejiang Sci-Tech University, Hangzhou 310018, China
[2] Hangzhou Aotuo Mechanical and Electrical Co. Ltd, Hangzhou 310018, China
[3] Key Laboratory of Special Purpose Equipment and Advanced Processing Technology, Ministry of Education and Zhejiang Province, College of Mechanical Engineering, Zhejiang University of Technology, Hangzhou 310023, China
[4] State Key Laboratory of Nonlinear Mechanics and Beijing Key Laboratory of Engineered Construction and Mechanobiology, Institute of Mechanics, Chinese Academy of Sciences, Beijing 100190, China

Received 18 January 2025 / Accepted 26 May 2025

Abstract Hydrogel-based actuators have shown great potential in the field of biomimetic soft robots due to their excellent flexibility and tunable mechanical properties. Despite considerable research efforts aimed at advancing hydrogel-based actuator technology, these actuators have not yet fully replicated the "recognition-judgment-execution" cycle characteristic of conscious, intelligent organisms, primarily due to the absence of integrated sensing mechanisms. To address this gap and mimic the intelligent actuation patterns of conscious organisms, we have developed an attractive soft actuator that combines substantial contraction capability with sensing functionality. This actuator innovatively integrates piezoresistive strain sensing and photo/thermal actuation functions within a single hydrogel material including gelatin, polyvinyl alcohol and MXene (GPM), enabling remote near-infrared (NIR) light-triggered actuation control. We propose a method of storing and releasing elastic potential energy, which can generate a high contraction force of up to 600 kPa, effectively overcoming the limitations of traditional osmosis-based actuation mechanisms in hydrogels. Moreover, the shape changes during actuation trigger the migration of MXene and significant alterations in the conductive network, endowing the GPM hydrogel with a wide sensing range (1–200% tensile strain), fast response time (191 ms), and excellent output signal linearity. Consequently, the actuator acquires self-sensing capabilities to monitor its deformation state in real time. Ultimately, inspired by the biological characteristics of snails, we designed an intelligent adaptive actuator capable of actively senseing external environmental stimuli and consciously adjusting its shape change accordingly. This integrated sensing-actuation hydrogel provides crucial insights and theoretical support for advancing artificial intelligence soft robots with higher autonomy and complexity.

1 Introduction

In the natural world, organisms are generally regarded as complex entities composed of multiple organ systems. Each organ system is responsible for specific functions, such as environmental perception, decision-making, mechanical movement execution, and information exchange [1–3]. With the continuous advancement of flexible electronics technology, flexible robots have garnered increasing attention due to their superior structural adaptability and high-efficiency interactive capabilities in dynamic environments [4, 5]. Fundamentally, organisms can be viewed as"soft robots"in nature, comprising various soft organs that have evolved to precisely perform their specialized functions. The materials, design principles, and operational mechanisms of these organisms serve as significant reference models for the development of soft robots [6–8]. Notably, the advancements in hydrogel technology has provided a substantial impetus to this field.

[a] e-mail: lilong@lnm.imech.ac.cn (corresponding author)
[b] e-mail: liuaiping1979@gmail.com (corresponding author)

Published online: 22 June 2025

When exposed to diverse external stimuli, biological organisms frequently demonstrate adaptive movements such as bending, folding, or twisting. These movements enable them to accomplish specific behavioral objectives, such as relocating to a preferred position or evading potential threats [9]. Such natural phenomena offer valuable insights for soft robotics research, especially in the development of stimulus-responsive materials like hydrogels [10, 11]. Hydrogel-based actuators can achieve substantial mechanical deformations through volume changes in response to specific external stimuli [12–15]. However, these hydrogel-based soft actuators typically exhibit purely reactive deformations without the sophisticated perception and control capabilities found intelligent biological sensory systems [16, 17]. For instance, snails can perceive the intensity of external stimuli and their own postures via neural activity, allowing them to adjust their movement patterns flexibly. In contrast, artificial hydrogel actuators lack the ability to make conscious judgment and control their deformations. This absence of feedback in the deformation pattern limits the adaptability and precision control of hydrogel actuators in complex and dynamic environments, thereby constraining their practical applications.

To further unlock the potential of artificial soft robots in practical applications, developing soft actuators that combine superior actuation performance with sensitive perception remains a critical research focus. In this study, we introduce a fast-actuating and self-sensing soft actuator based on an energy conversion mechanism. This conductive hydrogel features a double-network structure composed of polyvinyl alcohol (PVA) and gelatin (GA). MXene, a conductive material, endows the hydrogel with photo-thermal conversion capability and electrical conductivity (Fig. S1). The hydrogel integrates light/heat-driven actuation and strain sensing into a single material with a"two-in-one"function (Fig. 1a). Intriguingly, by incorporating a mechanism for storing and releasing elastic potential energy, the GA-PVA-MXene (GPM) hydrogel achieves impermeable actuation (Fig. 1b). When exposed to external stimuli, the hydrogel stores elastic potential energy through stretching and locking into a deformed state. Upon receiving new stimuli, the previously stored energy is rapidly released as the hydrogel rapidly contracts, resulting in rapid actuation and high force output. This process primarily consists of two key steps: (1) Due to the Hofmeister effect [18, 19], the gelatin chains and PVA chains can be immobilized via the formation of entangled regions of gelatin chains and crystalline domains of PVA chains, effectively locking the polymer chains in place. (2) Near-infrared (NIR) radiation and temperature changes can dissociate the triple helix structures and entanglement regions of gelatin chains as well as some crystalline domains of PVA chains [20]. During actuation, chain movement alters the MXene conductive network, resulting in measurable changes in the hydrogel's electrical properties, enabling real-time self-sensing. By leveraging this self-sensing capability, the GPM gel soft actuator can continuously monitor external stimuli and autonomously convert them into electrical signals, facilitating the system's environmental awareness. In summary, due to its confirmed high force output and precise self-sensing ability, this multifunctional actuating hydrogel offers innovative insights for the development of future autonomous soft robots.

2 Experimental section

2.1 Materials

Polyvinyl alcohol 1799 (PVA, hydrolyzed: > 99%) and Gelatin (gel strength ˜ 250 g Bloom) were provided by Shanghai McLain Biochemical Co., Ltd. (China). MXene was purchased from Shanghai Aladdin Biochemical Technology Co., Ltd. (China). All reagents were not further processed. Deionized water (ion exchange resin method, 18.2 MΩ at 25 °C) from Milli-Q Plus water purification system (Millipore) was used throughout the experiment.

2.2 Preparation of GPM

Gelatin powder (1.4 g) was added to 20 g of deionized water and stirred at 60 °C until a homogeneous solution was formed. Subsequently, PVA (5 g) was introduced into the solution, and the temperature was increased to 90 °C. Stirring was continued for 1.5 h to ensure complete dissolution of PVA, resulting in a homogeneous gelatin-PVA mixture. The resulting mixed solution was then cooled to 60 °C, after which the MXene aqueous dispersion was slowly added dropwise. Finally, the prepared solution was transferred into a custom-made mold, allowed to cool to room temperature, and subsequently stored in a freezer at −20 °C for 4 h to form the GPM gel. Similarly, Gelatin hydrogels, PVA hydrogels, and GA-PVA (GP) hydrogels were prepared following the same procedure.

2.3 Tensile strength test and calculation of output work density

This experiment quantified the actuation strength of GPM gel using a mechanical testing system. Initially, the dimensions of the sample were recorded, including the width (a_0), thickness (b_0), and length (l_0). Subsequently, the GPM gel was subjected to mechanical stretching to a displacement of 90 mm (corresponding to a strain of 200%).

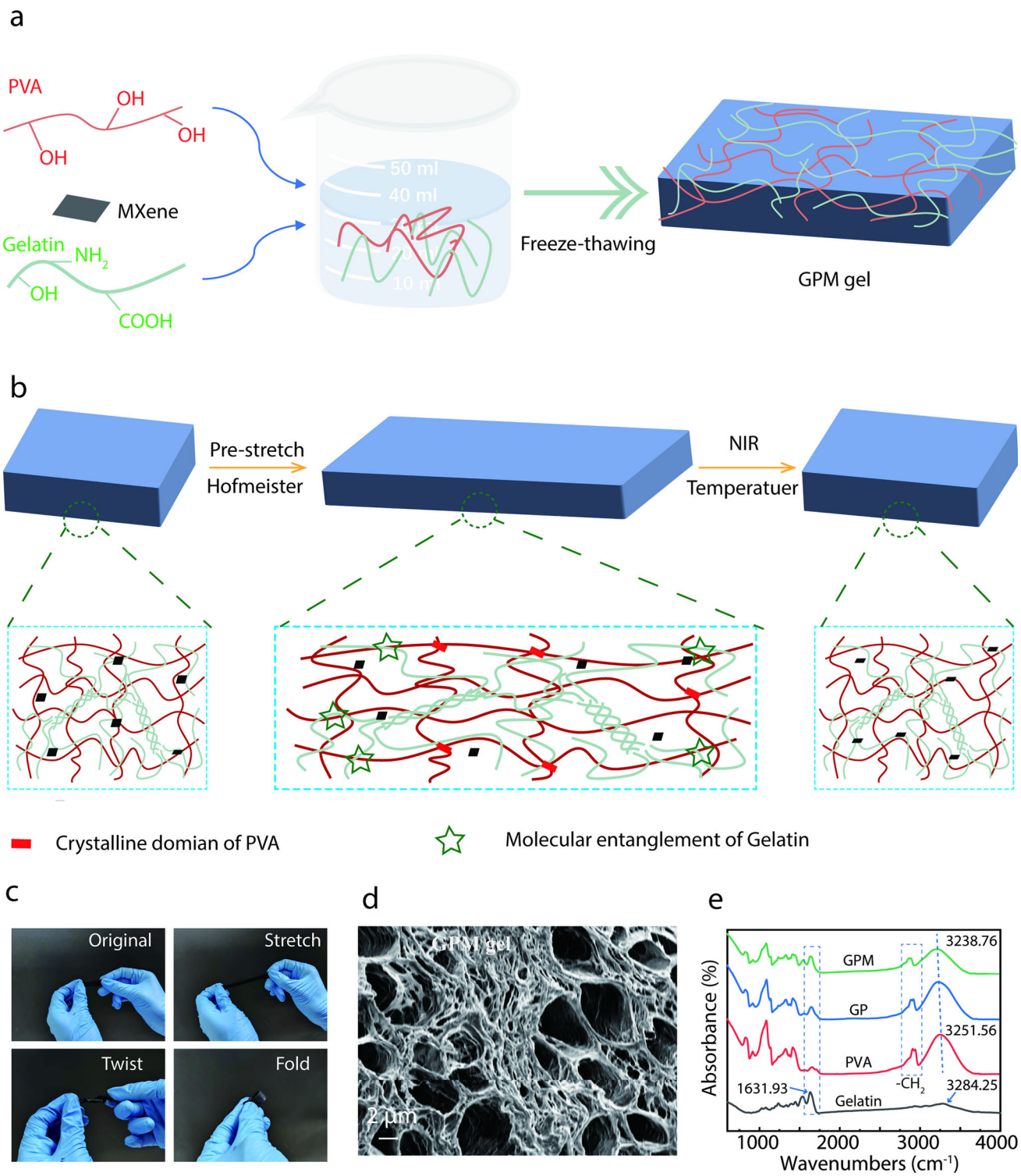

Fig. 1 GPM design ideas and basic performance. **a** Schematic illustration of the synthesis of GPM gel. **b** GPM is utilized as an actuator by the method of storing and releasing elastic potential energy. **c** The softness of GPM gel. **d** SEM image of GPM gel. **e** Fourier Transform Infrared spectra of Gelatin, PVA, GA-PVA (GP) and GA-PVA-MXene (GPM) gels

Next, the stored elastic potential energy of the GPM was quickly released by immersing it in 80 °C hot water, and the contraction force over time was monitored to generate the contraction strength-time curve. Following this, the sample holder was restored to the original length at a rate of 0.2 mm/s and the contraction force–displacement curve was recorded. Finally, the working energy density (W_E) was calculated using the formula $W_E = U_R/(a_0 * b_0 * l_0)$, where U_R is the total recovered energy from the sample.

2.4 Measurement and characterization

The Fourier Transform Infrared (FTIR) spectra in the range of 4000—400 cm^{-1} were recorded by an Infrared Spectrometer (Thermo Fisher Scientific, Nicolet iS50 series). Hydrogel samples were first frozen in liquid nitrogen and then lyophilized for 24 h to ensure complete removal of moisture. The morphology of the lyophilized hydrogels was observed by a Scanning Electron Microscope (S-4800, Hitachi, Tokyo, Japan). Tensile tests of the hydrogels at room temperature were recorded on a tensile testing machine (INSTRON, LEGEND 2366, USA), where the rectangular specimens were clamped at both ends and stretched at a rate of 20 $mm{\cdot}min^{-1}$. The electromechanical properties of the resistive sensor were evaluated in real-time using the Keithley 2400 dual-probe measurement system.

3 Results and discussion

3.1 Mechanical performance of GPM gel

Animals execute a wide range of effective movements through muscle contractions, including walking, swimming, and grasping objects [21, 22]. For an artificial actuator to accurately mimic these behaviors, it must possess the necessary softness, strength, and controllability to perform assigned tasks effectively. As depicted in Fig. 1c, the GPM gel exhibits high flexibility, capable of undergoing deformations such as stretching, twisting, and folding. Furthermore, the SEM image (Fig. 1d and Fig. S2) reveals a characteristic porous structure [23]. It is evident that the addition of gelatin also leads to a gradual decrease in the peak intensity of the methylene stretching vibration absorption (Fig. 1e). Additionally, the carbonyl characteristic peak is observed in the GPM gel [24]. These results suggest that strong hydrogen bonds have formed between polyvinyl alcohol and gelatin molecules, indicating good compatibility between the two polymers. Studies have demonstrated that different components significant influence the mechanical properties of GPM gel. We utilized Design-Expert V.12 statistical software and the Box-Behnken Design (BBD) method to design the experiments. The mass fractions of gelatin (A), PVA (B), and ammonium sulfate (C) were set as independent variables, while strain ($R1$) and stress ($R2$) were designated as dependent variables. A 3-factor 2-level response surface experiment was designed, with detailed experimental parameters presented in Table S1 (Supporting Information). When one of the three independent variables is maintained at the intermediate level, the projections of the other two variables form a series of concentric circles or ellipses, which represent the significance of their mutual influence. An elliptical curve indicates a significant interaction effect between the corresponding variables on the response value [25]. It can be observed from Fig. S3 that gelatin, PVA, and ammonium sulfate all have significant effects. The process was further optimized using response surface methodology. As illustrated in Fig. 2a, when the mass fractions of gelatin, PVA, and soaked ammonium sulfate are 7%, 25%, and 15%, respectively, the mechanical properties of the GP gel reach their optimal state. Mechanical properties are a critical factor for achieving high force output in hydrogels. Consequently, we conducted a quantitative analysis of the mechanical properties of GPM gel. The typical tensile stress–strain curves and the corresponding hysteresis loops are presented in Fig. 2b and c. With the incorporation of PVA and MXene, the mechanical properties of the hydrogel have been significantly enhanced. Specifically, the maximum stress of the GPM gel reaches 3.6 MPa, and the elongation at break is up to 550%. The improvement in mechanical properties of the GPM gel can be attributed to the increased crosslinking density. Firstly, compared to pure gelatin, the GPM gel exhibits higher crosslinking density through the triple helix and chain entanglement regions of gelatin chains as well as the crystalline domains of PVA chains [26, 27]. The increase in crosslinking density is also supported by the SEM images (Fig. S2), which show a reduction in pore size. Secondly, the functional groups on the surface of MXene provide additional crosslinking sites for the polymer chains [28]. Infrared spectroscopy further confirms the existence of intermolecular interactions, as evidenced by the shift in the stretching vibration peak of the hydroxyl group (Fig. 1e). The enhancement in mechanical properties is also reflected by the change in elastic modulus. The elastic moduli of pure gelatin and PVA gels are 0.1 MPa and 0.3 MPa, respectively, the GPM gel exhibits an elastic modulus of 1.3 MPa (Fig. 2d). Moreover, the fracture energy of the GPM gel is notably higher, facilitated by the entangled regions of polymer chains that enable effective load transfer between gelatin and PVA chains. Additionally, the gelatin's triple helix structure and the crystalline domains of PVA can dissociate, which allows for energy dissipation, ultimately leading to the GPM gel's superior fracture energy.

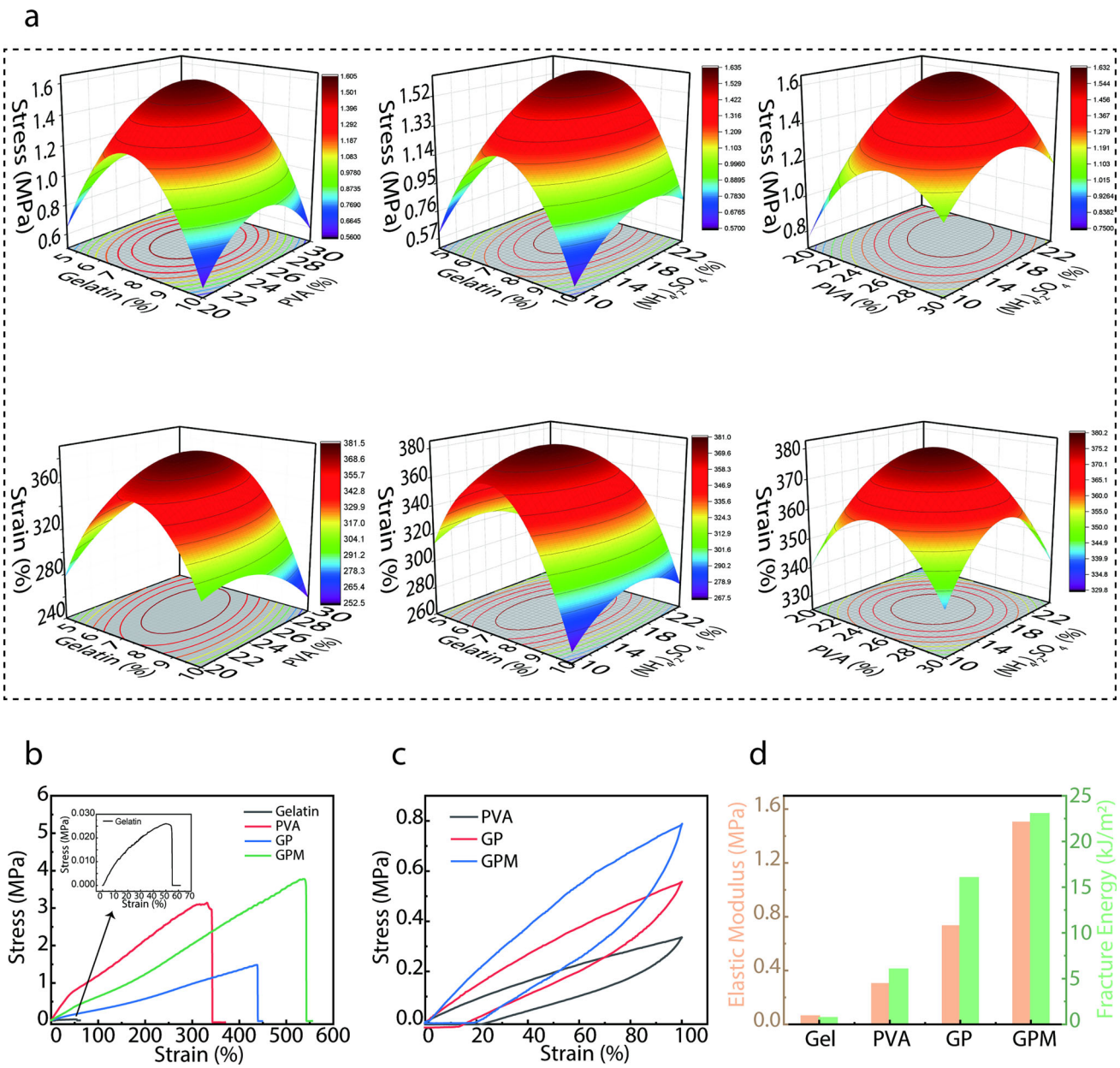

Fig. 2 Mechanical properties of GPM gels. **a** Response surface plot illustrating the interaction effects of various factors. **b** Tensile stress–strain curves of hydrogels with different compositions. **c** Typical tensile load-to-unload curves of hydrogels with different components. **d** Elastic modulus and fracture energy of hydrogels with different components

3.2 Sensing performance

As a soft machine, in addition to achieving high force output, self-sensing during actuation is equally critical. The embedded MXene imparts high conductivity to the GPM gel, enabling it to function as a strain sensor under mechanical deformation. Figure 3a demonstrates that when GPM gel is integrated into an electrical circuit, changes in the gel's length can modulate the brightness of a small bulb. Within the 0–200% tensile strain range, the gauge factor (GF = 3.2) is calculated based on the rate of change of $\Delta R/R_0$ with respect to strain, proving excellent sensitivity and linearity of sensor throughout the entire strain cycle (Fig. 3b). The response time of GPM gel was evaluated by instantaneously applying and abruptly removing a 10% strain (Fig. 3c). The results indicate that the response time is 422 ms, while the recovery time is merely 191 ms, which is comparable to typical hydrogel-based strain sensors [29, 30]. Furthermore, when the hydrogel is stretched to a preset strain, the $\Delta R/R_0$ increases proportionally with elongation. When the strain is maintained constant, $\Delta R/R_0$ remains stable, indicating the hydrogel's good electrical stability (Fig. 3d). Figure 3e further reveals the consistent relationship between resistance

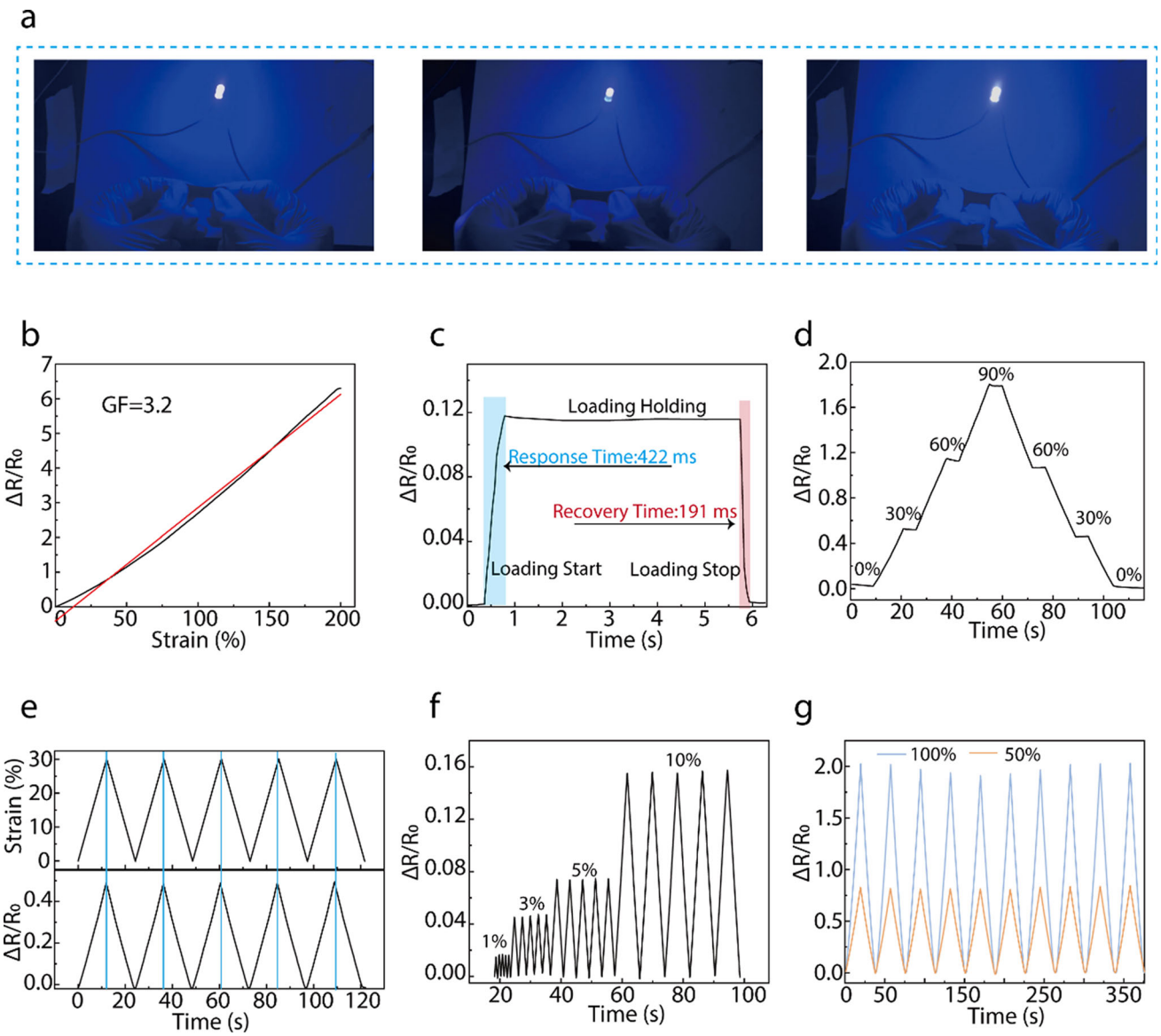

Fig. 3 Sensing performance of GPM gel. **a** Change the length of the GPM gel to control the brightness of the small bulb. **b** Relative resistance change of GPM gel conductive hydrogels under stretching. **c** Response time of GPM gel sensor. **d** Relative resistance change under step strains. **e** Relative resistance changes in real time with strain. Relative resistance changes at different frequencies with small strain (**f**) and large strain (**g**)

change and strain. Figure 3f, g, and S4 showcase the reproducibility and reliability of the sensor's electrical signal values under various cyclic strains, including both small strains (< 10%) and large strains. Its rapid response and outstanding reversibility make it valuable for real-time monitoring of deformation in response to external stimuli. For instance, when attached to human joints, the GPM gel sensor can provide timely feedback on human physiological signals (Fig. S5).

3.3 Actuation mechanism of GPM gel

The fundamental capability of GPM to generate high force lies in its ability to overcome the inherent limitations of the traditional hydrogel osmotic-driven mechanism. Specifically, GPM gel employs the storage and release of elastic potential energy as its actuation method. As depicted in Fig. 4a, initially, GPM gel is mechanically stretched and immersed in 15 wt% $(NH_4)_2SO_4$. During this process, the Hofmeister effect [31] induces the formation of entangled regions within the gelatin chains and crystalline domains in the PVA chains, effectively locking the polymer chains and fixing the gel in its stretched configuration, thereby storing elastic potential energy (EPE). Upon actuation,

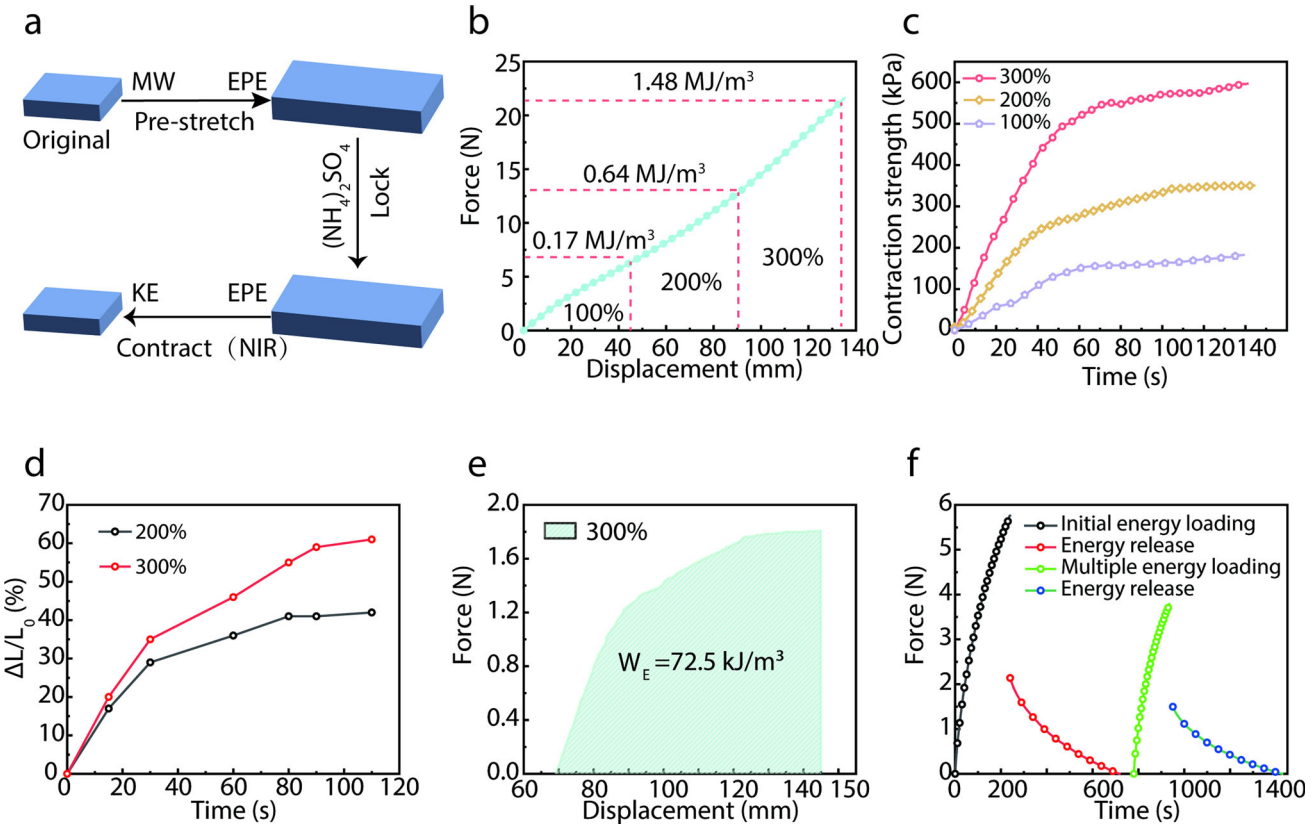

Fig. 4 GPM gel utilizes an actuating mechanism that stores and releases elastic potential energy. **a** Schematic diagram of energy conversion process in GPM gel. **b** Elastic energy density as a function of pre-stretch ratio due to mechanical work (MW). **c** Contraction strength of hydrogels with varying pre-tensioning ratios. **d** The length change ratio of GPM gel (where ΔL was the length change, L_0 was the initial length) at different fixed strains as a function of stimulation time. **e** Output working density of GPM gel under fixed strain of 300%. **f** Multiple energy storage and release cycles of GPM gel

when exposed to either 80 °C hot water or near-infrared light, the GPM gel undergoes rapid contraction. This process converts the stored elastic potential energy into kinetic energy (KE) of the GPM. The contraction is triggered by the disruption of the triple helix structure and entanglement regions of the gelatin chains, as well as the dissociation of certain crystalline domains in the PVA chains. Further quantitative studies have been conducted to examine the elastic potential energy that can stored by GPM gel. Results show that as the mechanical stretching length increases, so does the stored energy, reaching a maximum of 1.48 MJ/m^3 (Fig. 4b). It is reasonable to predict that a higher stored energy correlates with a greater contraction force upon release; however, the energy trapped in the entangled regions of gelatin chains and the crystalline domains of PVA chains remain limited. As illustrated in Fig. 4c, GPM gel can generate a maximum contraction force of up to 600 kPa. Additionally, the length change of the GPM gel during the contraction process was investigated. As shown in Fig. 4d, the length change rates of different samples increase with stimulation time, ultimately reaching 41% and 60%, respectively, within 100 s. This demonstrates that GPM gel with varying levels of fixed strain exhibit significant length changes during actuation. To quantify the output work density, the elastic potential energy released during the network unlocking process was calculated based on the force–displacement curve obtained during contraction. Figure 4e illustrates the elastic potential energy released by the GPM gel with fixed strain during this network unlocking process. The entire actuation process generates approximately 1.75 N of contraction force and an output work density of 72.5 kJ/m^3. To verify the stability of the actuation process, multiple actuation experiments were conducted. The superior photothermal conversion performance of MXene ensures the stability of NIR control (Fig. S6). Furthermore, as depicted in Fig. 4f, after multiple actuations, the generated actuation force exhibits a slight decrease. This reduction is attributed to the weakening of the mechanical properties of the GPM gel due to repeated mechanical stretching (Fig. S7).

3.4 Somatosensory actuation

Owing to its superior force driving and sensing capabilities, GPM gel holds extensive potential for manufacturing flexible actuators. By adopting specific structural configurations, GPM gel can be engineered into functional actuating devices. For instance, as depicted in Fig. 5a, the GPM gel contracts upon exposure to 80 °C hot water, effectively lifting a target object weighing approximately 10 g. Additionally, the motion state of GPM gel can be monitored through variation in electrical signals (Fig. 5b). Furthermore, when integrated with a robotic hand,

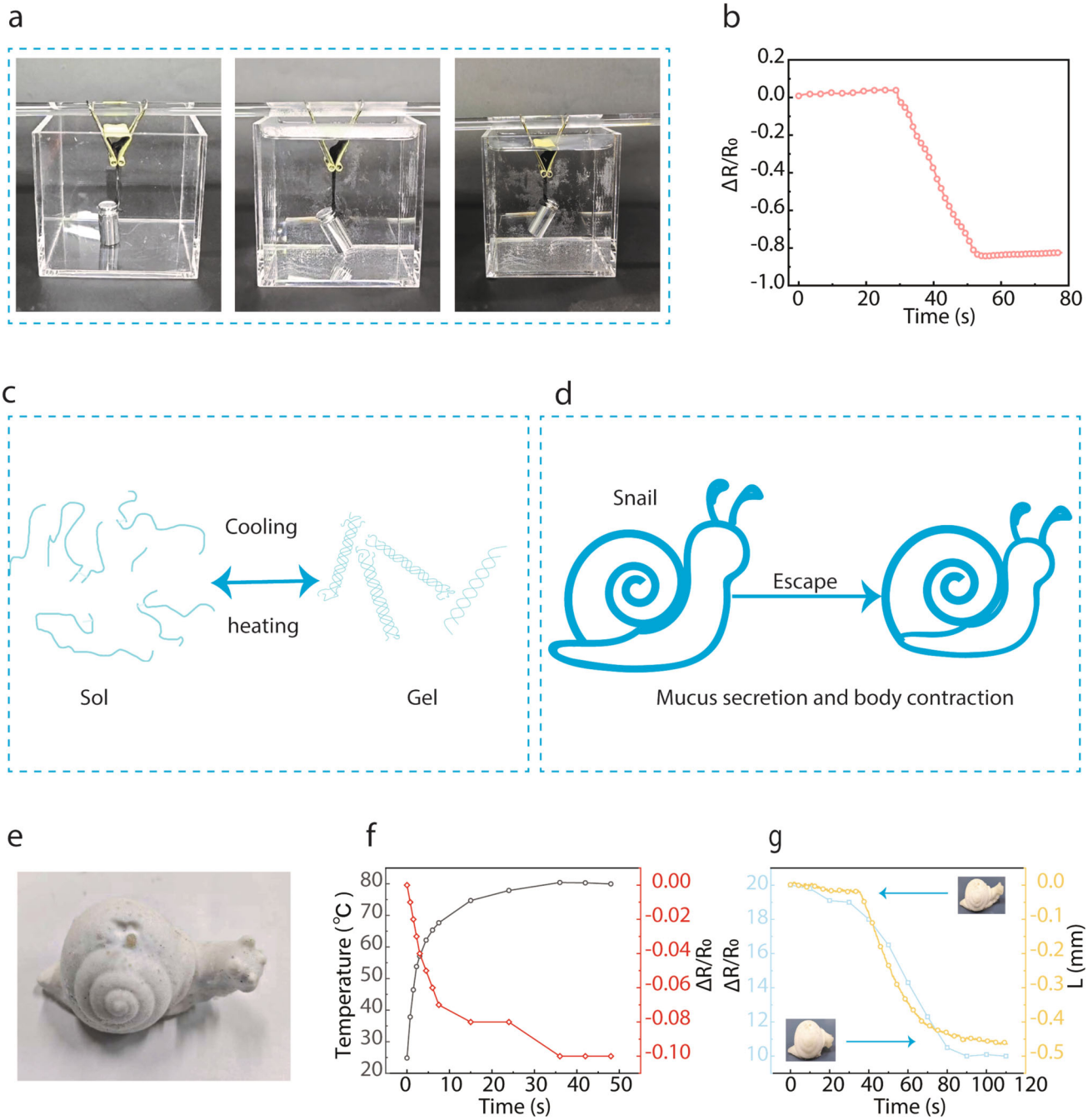

Fig. 5 GPM gel exhibits remarkable actuation and sensing capability. **a** Photographs of GPM gel successfully lifting 10 g weight load under stimulation, along with real-time electrical signal changes during deformation (**b**). **c** Sol–gel conversion of gelatin. **d** A schematic diagram of a snail escaping from danger. **e** The PGM gel molded into the shape of a snail. **f** The relationship between temperature and relative resistance in the GPM gel sensor. **g** Real-time variations in electrical signals during GPM gel movement

it can facilitate various gestures and movements (Fig. S8). Notably, GPM gel exhibits specific responsiveness to temperature stimuli. Specifically, it undergoes length change and forms a sol layer on its surface due to the inherent sol–gel transformation property of gelatin [32]. This sol layer significantly reduces surface friction between the GPM gel and other objects (Fig. 5c). Figure 5d illustrates the escape mechanism of a snail in response to danger. In nature, when a snail is subjected to external environment, it assesses the intensity of the external stimulus and its own posture through neural activities, rapidly secretes mucus to reduce the friction with the predator, and contracts its body to escape capture. Similarly, when we fabricate the GPM gel into a snail-like shape, a comparable movement process can be observed (Fig. 5e). We initially investigated the influence of temperature on the resistance of GPM gel. As shown in Fig. 5f, upon NIR stimulation, the temperature of the GPM gel gradually increases, leading to a slight decrease in its resistance. The rise in temperature enhances the thermal motion of electrons and holes on the surface of MXene, allowing more carriers to break free from covalent bonds [33]. From Fig. 5g, it is evident that when a near-infrared beam irradiates the snail-shaped GPM gel, inducing its photothermal-mechanical motion, a significant drop in resistance occurs in the corresponding circuit. Additionally, the change in length can also be determined by monitoring the real-time feedback electrical signal in the circuit. In other words, by tracking the feedback electrical signal, the real-time deformation degree during the actuation process of the GPM actuator can be identified.

4 Conclusion

In conclusion, this work presents a photothermal-responsive soft actuator based on a double-network composite hydrogel of GA/PVA/MXene, featuring high driving force and self-sensing capability. An innovative actuation method leveraging the storage and release of elastic potential energy is proposed. The reversible chain entanglement regions of gelatin chains and the crystallization domains of PVA chains serve as switches for energy conversion, enabling precise and controllable energy transformation. This mechanism results in significant contraction forces during the actuation process. Benefiting from the superior conductivity and photothermal conversion capacity of MXene, the GPM gel achieves remote control capabilities. Under localized near-infrared (NIR) irradiation, the local temperature changes induced by MXene's photothermal effect enable the proposed soft actuator to perform rapid, adjustable and programmable movements within seconds Moreover, the conductive network of MXene endows the GPM soft actuator with real-time self-sensing ability. During the actuation process, the movement of the polymer chains generates a strong deformation-electric correlation, facilitated by the MXene conductive network. This integrated design of perception and actuation provides valuable inspiration and a robust theoretical foundation for the development of advanced autonomous and multifunctional artificial intelligent soft robots. The findings pave the way for future advancements in soft robotics, enabling more sophisticated and adaptable systems capable of mimicking biological behaviors with enhanced precision and autonomy.

Supplementary Information The online version contains supplementary material available at https://doi.org/10.1140/epjs/s11734-025-01713-w.

Acknowledgements This work was supported by the National Natural Science Foundation of China (No. 12272351, 62401509 and 12372168), the National Key Research and Development Program of China (2024YFB3816500), the Zhejiang Provincial Natural Science Foundation of China (No. LZ24A020004 and LRG25A020001), the Youth Innovation Promotion Association CAS, the National Key Research and Development Program of China (2024YFB3816500).

Author contributions

Ping Guo: Methodology, Data curation, Writing-Original draft preparation; Yingqiang Zhou: Data curation, Software, Validation; Wenjie Cao: Data curation, Software; Xinyin Wang: Software, Validation; Tian Wang: Software, Validation; Hongxiang Su: Software, Validation; Lin Cheng: Formal analysis, Investigation; Huaping Wu: Formal analysis, Investigation; Long Li: Investigation; Aiping Liu: Supervision, Conceptualization, Methodology, Writing-review & editing.

Data availability Available on request.

Declarations

Conflict of interest The authors declare that they have no known competing financial interests or personal relationships that could have appeared to influence the work reported in this paper.

Supporting information Including the preparation process, contour map, SEM, electrical testing, motion signal detection, MXene photothermal performance, mechanical properties before and after energy conversion, and more data and figures.

References

1. L.N. Vandenberg, D.S. Adams, M. Levin, Normalized shape and location of perturbed craniofacial structures in the Xenopus tadpole reveal an innate ability to achieve correct morphology. Dev Dynam **241**(5), 863–878 (2012). https://doi.org/10.1002/dvdy.23770
2. C.S. Park, Y.W. Kang, H. Na, J.Y. Sun, Hydrogels for bioinspired soft robots. Prog. Polym. Sci. **150**, 101791 (2024). https://doi.org/10.1016/j.progpolymsci.2024.101791
3. T.B.H. Schroeder, A. Guha, A. Lamoureux, G. VanRenterghem, D. Sept, M. Shtein, J. Yang, M. Mayer, An electric-eel-inspired soft power source from stacked hydrogels. Nature **552**(7684), 214–218 (2017). https://doi.org/10.1038/nature24670
4. D. Rus, M.T. Tolley, Design, fabrication and control of soft robots. Nature **521**(7553), 467–475 (2015). https://doi.org/10.1038/nature14543
5. R. Nasseri, N. Bouzari, J.T. Huang, H. Golzar, S. Jankhani, X.W. Tang, T.H. Mekonnen, A. Aghakhani, H. Shahsavan, Programmable nanocomposites of cellulose nanocrystals and zwitterionic hydrogels for soft robotics. Nat. Commun. **14**(1), 6108 (2023). https://doi.org/10.1038/s41467-023-41874-7
6. J.C. Yeo, H.K. Yap, W. Xi, Z.P. Wang, C.H. Yeow, C.T. Lim, Flexible and Stretchable Strain Sensing Actuator for Wearable Soft Robotic Applications. Adv Mater Technol **1**(3), 1600018 (2016). https://doi.org/10.1002/admt.201600018
7. Z. Chen, H.G. Wang, Y.T. Cao, Y.J. Chen, O. Akkus, H.Z. Liu, C.Y. Cao, Bio-inspired anisotropic hydrogels and their applications in soft actuators and robots. Matter **6**(11), 3803–3837 (2023). https://doi.org/10.1016/j.matt.2023.08.011
8. Z.C. Wang, X. Zhang, Y. Wang, Z.Y. Fang, H. Jiang, Q.L. Yang, X.F. Zhu, M.Z. Liu, X.D. Fan, J. Kong, Untethered Soft Microrobots with Adaptive Logic Gates. Adv. Sci. **10**(13), 2206662 (2023). https://doi.org/10.1002/advs.202206662
9. H.B. Wang, M. Totaro, L. Beccai, Toward Perceptive Soft Robots: Progress and Challenges. Adv. Sci. **5**(9), 1800541 (2018). https://doi.org/10.1002/advs.201800541
10. Y.F. Ma, M.T. Hua, S.W. Wu, Y.J. Du, X.W. Pei, X.Y. Zhu, F. Zhou, X.M. He, Bioinspired high-power-density strong contractile hydrogel by programmable elastic recoil, Sci Adv 6(47) (2020) eabd2520. https://doi.org/10.1126/sciadv.abd2520.
11. Y. Lee, W.J. Song, J.Y. Sun, Hydrogel soft robotics. Mater Today Phys **15**, 100258 (2020). https://doi.org/10.1016/j.mtphys.2020.100258
12. Z. Jiang, M.L. Tan, M. Taheri, Q. Yan, T. Tsuzuki, M.G. Gardiner, B. Diggle, L.A. Connal, Strong. Self-Healable, and Recyclable Visible-Light-Responsive Hydrogel Actuators, Angew Chem Int Edit **59**(18), 7049–7056 (2020). https://doi.org/10.1002/anie.201916058
13. S. Li, W.H. Wang, W.T. Li, M.F. Xie, C.X. Deng, X. Sun, C.W. Wang, Y. Liu, G.H. Shi, Y.J. Xu, X.J. Ma, J.W. Wang, Fabrication of Thermoresponsive Hydrogel Scaffolds with Engineered Microscale Vasculatures. Adv. Funct. Mater. **31**(27), 2102685 (2021). https://doi.org/10.1002/adfm.202102685
14. E. Wang, M.S. Desai, S.W. Lee, Light-Controlled Graphene-Elastin Composite Hydrogel Actuators. Nano Lett. **13**(6), 2826–2830 (2013). https://doi.org/10.1021/nl401088b
15. X.Y. Ding, W.Z. Li, L.R. Shang, Y.J. Zhao, W.J. Sun, Controllable Contact-Destructive Hydrogel Actuators. Adv. Mater. **36**(45), 2409965 (2024). https://doi.org/10.1002/adma.202409965
16. Y.S. Zhao, C.Y. Lo, L.C. Ruan, C.H. Pi, C. Kim, Y. Alsaid, I. Frenkel, R. Rico, T.C. Tsao, X.M. He, Somatosensory actuator based on stretchable conductive photothermally responsive hydrogel, Sci Robot 6(53) (2021) eabd5483. https://doi.org/10.1126/scirobotics.abd5483.
17. X.C. Cui, Z.Z. Liu, B. Zhang, X.D. Tang, F.Q. Fan, Y. Fu, J.H. Zhang, T.Q. Wang, F.B. Meng, Sponge-like, semi-interpenetrating self-sensory hydrogel for smart photothermal-responsive soft actuator with biomimetic self-diagnostic intelligence. Chem. Eng. J. **467**, 143515 (2023). https://doi.org/10.1016/j.cej.2023.143515
18. M.T. Hua, S.W. Wu, Y.F. Ma, Y.S. Zhao, Z.L. Chen, I. Frenkel, J. Strzalka, H. Zhou, X.Y. Zhu, X.M. He, Strong tough hydrogels via the synergy of freeze-casting and salting out. Nature **590**(7847), 594–599 (2021). https://doi.org/10.1038/s41586-021-03212-z
19. Y. Zhang, Y.S. Xiong, X.S. Li, S.H. Zhang, W.L. Xu, H. Chen, L. Xu, Oxidization and Salting Out Synergistically Induced Highly Elastic, Conductive, and Sensitive Polyvinyl Alcohol Hydrogels, Adv Funct Mater (2024) 2415207. https://doi.org/10.1002/adfm.202415207.
20. C.L. Liu, H.J. Zhang, X.Y. You, K.P. Cui, X.C. Wang, Electrically Conductive Tough Gelatin Hydrogel. Adv Electron Mater **6**(4), 2000040 (2020). https://doi.org/10.1002/aelm.202000040
21. C.H. Qian, Y.Q. Li, C. Chen, L. Han, Q.S. Han, L.K. Liu, Z.C. Lu, A stretchable and conductive design based on multi-responsive hydrogel for self-sensing actuators. Chem. Eng. J. **454**, 140263 (2023). https://doi.org/10.1016/j.cej.2022.140263
22. S.S. Ma, P. Xue, C. Valenzuela, X. Zhang, Y.H. Chen, Y. Liu, L. Yang, X.H. Xu, L. Wang, Highly Stretchable and Conductive MXene-Encapsulated Liquid Metal Hydrogels forBioinspired Self-Sensing Soft Actuators. Adv. Funct. Mater. **34**(7), 2309899 (2024). https://doi.org/10.1002/adfm.202309899

23. Z.H. Li, Z.W. Li, S.H. Zhou, J.M. Zhang, L. Zong, Biomimetic Multiscale Oriented PVA/NRL Hydrogel Enabled Multistimulus Responsive and Smart Shape Memory Actuator. Small **20**(25), 2311240 (2024). https://doi.org/10.1002/smll.202311240
24. H. Jeong, D.Y. Lee, D.H. Yang, Y.S. Song, Mechanical and Cell-Adhesive Properties of Gelatin/Polyvinyl Alcohol Hydrogels and Their Application in Wound Dressing. Macromol. Res. **30**(4), 223–229 (2022). https://doi.org/10.1007/s13233-022-0027-7
25. A.I. Alateyah, M. El-Shenawy, A. Nassef, M. El-Hadek, M.M.Z. Ahmed, H. Kouta, S. El Sanabary, W.H. El-Garaihy, Optimizing the ECAP processing parameters of pure Cu through experimental, finite element, and response surface approaches. Rev. Adv. Mater. Sci. **62**(1), 20220297 (2023). https://doi.org/10.1515/rams-2022-0297
26. X.W. Xu, V.V. Jerca, R. Hoogenboom, Bioinspired double network hydrogels: from covalent double network hydrogels hybrid double network hydrogels to physical double network hydrogels. Mater. Horiz. **8**(4), 1173–1188 (2021). https://doi.org/10.1039/d0mh01514h
27. S.M. Hu, Y.H. Fang, C. Liang, M. Turunen, O. Ikkala, H. Zhang, Thermally trainable dual network hydrogels. Nat. Commun. **14**(1), 3717 (2023). https://doi.org/10.1038/s41467-023-39446-w
28. X.X. Luo, L.P. Zhu, Y.C. Wang, J.Y. Li, J.J. Nie, Z.L. Wang, A Flexible Multifunctional Triboelectric Nanogenerator Based on MXene/PVA Hydrogel. Adv. Funct. Mater. **31**(38), 2104928 (2021). https://doi.org/10.1002/adfm.202104928
29. R.N. Liu, Y.Y. Liu, S.M. Fu, Y.G. Cheng, K.M. Jin, J.T. Ma, Y.C. Wan, Y. Tian, Humidity Adaptive Antifreeze Hydrogel Sensor for Intelligent Control and Human-Computer Interaction. Small **20**(24), 2308092 (2024). https://doi.org/10.1002/smll.202308092
30. P. Guo, Z.X. Zhang, C.N. Qian, R.F. Wang, L. Cheng, Y. Tian, H.P. Wu, S.Z. Zhu, A.P. Liu, Programming Hydrogen Bonds for Reversible Elastic-Plastic Phase Transition in a Conductive Stretchable Hydrogel Actuator with Rapid Ultra-High-Density Energy Conversion and Multiple Sensory Properties. Adv. Mater. **36**(46), 2410324 (2024). https://doi.org/10.1002/adma.202410324
31. X.J. Wang, C.D. Qiao, S. Jiang, L.B. Liu, J.S. Yao, Hofmeister effect in gelatin-based hydrogels with shape memory properties. Colloid Surface B **217**, 112674 (2022). https://doi.org/10.1016/j.colsurfb.2022.112674
32. M. Helminger, B.H. Wu, T. Kollmann, D. Benke, D. Schwahn, V. Pipich, D. Faivre, D. Zahn, H. Cölfen, Synthesis and Characterization of Gelatin-Based Magnetic Hydrogels. Adv. Funct. Mater. **24**(21), 3187–3196 (2014). https://doi.org/10.1002/adfm.201303547
33. Y. Wei, L.J. Xiang, H.J. Ou, F. Li, Y.Z. Zhang, Y.Y. Qian, L.J. Hao, J.J. Diao, M.L. Zhang, P.H. Zhu, Y.J. Liu, Y.D. Kuang, G. Chen, MXene-Based Conductive Organohydrogels with Long-Term Environmental Stability and Multifunctionality. Adv. Funct. Mater. **30**(48), 2005135 (2020). https://doi.org/10.1002/adfm.202005135